

Published in final edited form as:

Osteoarthritis Cartilage. 2011 July ; 19(7): 911–918. doi:10.1016/j.joca.2011.03.002.

Regional Cell Density Distribution and Oxygen Consumption Rates in Porcine TMJ Discs: An Explant Study

Jonathan Kuo¹, Changcheng Shi¹, Sarah Cisewski¹, Lixia Zhang², Michael J. Kern², and Hai Yao^{1,2}

¹ Department of Bioengineering, Clemson University, Clemson, SC

² Department of Craniofacial Biology, Medical University of South Carolina (MUSC), Charleston, SC

Abstract

Objective—To determine the regional cell density distribution and basal oxygen consumption rates (based on tissue volume and cell number) of temporomandibular joint (TMJ) discs and further examine the impact of oxygen tension on these rates.

Design—TMJ discs from pigs aged 6–8 months were divided into five regions: anterior, intermediate, posterior, lateral and medial. The cell density was determined using confocal laser scanning microscopy. The change in oxygen tension was recorded while TMJ disc explants were cultured in sealed metabolism chambers. The volume based oxygen consumption rate of explants was determined by theoretical curve fitting of the recorded oxygen tension data with the Michaelis-Menten equation. The rate on a per-cell basis was calculated based on the cell density measurements and volume based rate measured in another group of discs.

Results—The overall cell density (mean, 95% CI) was $51.3(21.3–81.3) \times 10^6$ cells/mL wet tissue. Along the anteroposterior axis, the anterior band had 25.5% higher cell density than the intermediate zone ($p < 0.02$) and 29.1% higher than the posterior band ($p < 0.008$). Along the mediolateral axes, the medial region had 26.2% higher cell density than the intermediate zone ($p < 0.04$) and 25.4% higher than the lateral region ($p < 0.045$). The overall volume and cell based maximum oxygen consumption rates were $1.44(0.44–2.44)$ $\mu\text{mol/mL}$ wet tissue/hr and $28.7(12.2–45.2)$ $\text{nmol}/10^6$ cells/hr, respectively. The central regions (intermediate, lateral, and medial) had significantly higher volume based ($p < 0.02$) and cell based ($p < 0.005$) oxygen consumption rates than the anterior and posterior bands. At high oxygen tension, the oxygen consumption rate remained constant, but dropped as oxygen tension fell below 5%.

© 2011 OsteoArthritis Society International. Published by Elsevier Ltd. All rights reserved.

Address for Correspondence: Hai Yao, PhD, Department of Bioengineering, Clemson University, Clemson-MUSC Bioengineering Program, 173 Ashley Avenue, P.O. Box 250508, Charleston, SC 29425, Phone: (843)792-2365, Fax: (843)792-9946, haiyao@clemson.edu.

AUTHOR CONTRIBUTIONS

The authors made substantial contributions in designing the study (JK, MJK, HY), gathering and analyzing the data (JK, CS, SC, LZ, HY), and drafting the article (JK, MJK, HY).

CONFLICT OF INTEREST

None of the authors of this paper have a conflict of interest that might be construed as affecting the conduct or reporting of the work presented.

Publisher's Disclaimer: This is a PDF file of an unedited manuscript that has been accepted for publication. As a service to our customers we are providing this early version of the manuscript. The manuscript will undergo copyediting, typesetting, and review of the resulting proof before it is published in its final citable form. Please note that during the production process errors may be discovered which could affect the content, and all legal disclaimers that apply to the journal pertain.

Conclusions—The TMJ disc had higher cell density and oxygen consumption rates than articular cartilage reported in the literature. These results suggest that a steeper oxygen gradient may exist in the TMJ disc and may be vulnerable to pathological events that impede nutrient supply.

Keywords

Temporomandibular joint (TMJ) disc; Cell density distribution; Oxygen consumption rate; Metabolism

INTRODUCTION

The temporomandibular joint (TMJ) is a synovial, bilateral joint with unique morphology and function. The TMJ disc, a fibrocartilaginous tissue, is a major component of jaw function by providing stress distribution and lubrication in the joint^{1–2}. Disc derangement (e.g., dislocation of the disc) is a common clinical finding in patients with TMJ disorders (affecting more than 10 million Americans)³. It has been suggested that degenerative processes predispose the disc to displacement and result in significant changes in disc morphology, biochemistry, material properties, and function^{3–4}.

The normal adult human TMJ disc is a large avascular structure^{5–7}, so the nutrients required by disc cells for maintaining disc health are supplied by synovial fluid at the margins of the disc as well as through nearby blood vessels at the connection to the posterior bilaminar zone⁸. The transport of small nutrients (i.e., oxygen and glucose) within the TMJ disc mainly depends on diffusion. The balance between the rate of nutrient diffusion through the matrix and the rate of consumption by disc cells potentially establishes a concentration gradient within the disc. In articular cartilage, these gradients can profoundly affect chondrocyte viability, energy metabolism, matrix synthesis, and response to inflammatory factors^{9–16}. Recent studies have shown that hypoxia with inflammation modulates gene expressions of tenascin-C and matrix metalloproteinases in TMJ disc cells^{17–18}. Understanding these gradients is therefore important for studying TMJ disc physiology and pathophysiology. Due to the difficulty of measuring these gradients *in vivo*, mathematical models have been used to predict the nutrient environment inside cartilaginous tissues. Most of these models have primarily studied oxygen as it is regarded as an important factor directly affecting cell biological activity¹⁴. Oxygen gradients have been modeled for growth cartilage¹⁹, articular cartilage²⁰, engineered cartilage^{21–22} and the intervertebral disc (IVD)^{23–24}. In order to obtain a realistic prediction of *in vivo* nutrient distribution, metabolic rates of cells have to be taken into account in the theoretical model. Therefore, measuring the oxygen consumption rate of TMJ disc cells is crucial for precise theoretical analyses of nutrient transport in the TMJ disc. Moreover, oxygen consumption data will provide useful information for understanding the mechanism of the energy metabolism of TMJ disc cells.

On a per-cell basis, the oxygen consumption rate of articular cartilage and IVD are remarkably lower than vascularized tissues (~ 2–5% of liver or kidney tissue rates)²⁵ since articular chondrocytes^{14, 26} and IVD cells²⁷ obtain their energy primarily through glycolysis. The rates of oxygen consumption in articular cartilage^{20, 28} and IVD^{29–30} depend on the local oxygen tension. The consumption of oxygen decreases as oxygen tension decreases and is regionally dependent. The deep zone articular chondrocytes had higher oxygen consumption rates than superficial zone cells²⁸. In IVD, the nucleus pulposus cells have a higher rate than annulus fibrosus cells^{30–32}. Compared to articular cartilage and other fibrocartilaginous tissues (e.g., IVD or knee meniscus), the TMJ disc has a unique matrix composition and cell phenotype^{33–35}. Differences in biochemical composition and structure distinguish three regions of the TMJ disc: anterior band, intermediate zone, and posterior

band⁵. Based on the cell morphological studies it appears that the TMJ disc contains an inhomogeneous distribution of a mixed cell population of fibroblast-like cells and chondrocyte-like cells, which are distinct from chondrocytes from hyaline cartilage³⁶. These differences imply that the nutrient consumption rate in the TMJ disc may be region-dependent and different from the rates of articular cartilage. However, to our knowledge the oxygen consumption rate of the TMJ disc has not been investigated.

The objective of this paper was to determine basal oxygen consumption rates in each porcine TMJ disc region and further examine the impact of oxygen tension on these rates. The oxygen consumption in a tissue depends on the cell density and oxygen consumption rate per cell, so both were experimentally determined in this study. The volume based *in situ* TMJ disc cell density distribution was established using confocal laser scanning microscopy. Next, oxygen consumption rates (on a per tissue volume basis) were determined at various oxygen tensions for TMJ disc explants. The oxygen consumption rates on a per-cell basis were finally calculated based on the independently measured cell density and volume based tissue oxygen consumption rate.

MATERIALS AND METHOD

Specimen preparation

A total of nine pig heads (American Yorkshire, male, aged ~ 6–8 months) were collected from a local abattoir within 2 hours of slaughter. The entire TMJ with capsule intact was removed *en bloc*. Joints were opened under a sterile dissection hood; TMJ discs were then removed and washed with 5–6 changes of phosphate buffered saline. Five TMJ discs of the left joints were used to determine cell density distribution via confocal laser scanning microscopy. Five TMJ discs of the corresponding right joints were used to determine DNA content to validate cell density measurements. Eight discs from both left and right joints were then used to measure the oxygen consumption rate of tissue explants.

Cell density measurement

A confocal microscopy based technique was developed to determine the *in situ* surface-regional cell distribution of the TMJ disc. The volume-based cell density measurements were accomplished by counting cell numbers in specific volumes from reconstructed three-dimensional (3D) images. Each porcine TMJ disc was divided into five regions: anterior, intermediate, posterior, lateral and medial [Fig. 1(A)]. These specimens were then sectioned into three layers (100 μ m each) along the superior-inferior axis using a microtome (SM2400, Leica Microsystems GmbH, Wetzlar, Germany). The nuclei of samples were stained with DRAQ5TM (Biostatus Limited, Leicestershire, UK) and all samples then were scanned with a Leica TCS SP5 Confocal Microscope System (Leica Microsystems, Inc., Exton, PA). 2D image series were acquired by Z-stack scanning with a 1 μ m step in the Z-direction and a Field of View in the X-Y plane of 387.5 μ m \times 387.5 μ m. 3D images of stained cells were reconstructed in the image processing software based on the Z-stack image series, and cell density measurements were obtained from these by counting cell numbers in observed tissue volumes [Fig. 1(B)].

DNA content measurement

The above technique was validated by measuring the DNA content of corresponding disc tissues from the same animals. Tissue plugs were punched from five regions of the right side discs, and the volume of each specimen was determined in PBS using a density determination kit (Sartorius YDK01, Germany) and an analytical balance based on the Archimedes' principle³⁷. The specimens were lyophilized for 2 days and then digested in 1 mL of papain solution (125 μ g/ml papain; Worthington Biomedical Corporation), 100 mM

phosphate buffer, 10 mM cysteine and 10 mM EDTA, at pH 6.3 and 60°C for 36 hours. The DNA content was determined using a DNA Quantitation Kit, Fluorescence Assay (Sigma, St. Louis, MO, USA). A conversion factor of 7.7 pg DNA per TMJ disc cell was used³⁸. The cell density of the specimen was determined by taking the ratio of cell number to tissue volume.

Oxygen consumption rate measurement

Fresh TMJ disc explants (~0.075g wet weight/explant) were harvested from 5 regions and the tissue volume of each explant was determined in PBS based on the Archimedes' principle using the previously described method. Explants were immediately diced into small pieces to minimize the concentration gradient of oxygen within the explant and then placed into a metabolism chamber containing DMEM with 5mM glucose at pH 7.4. This glucose concentration is considered physiological in synovial fluid²⁶ and was selected for measuring basal oxygen consumption rate of the TMJ disc in this study. The medium used in the metabolism chamber had been preheated to 37 °C and stirred in air for 10 minutes to establish constant initial dissolved oxygen concentration. The concentration of dissolved oxygen in the culture medium at 37°C and atmospheric pressure was 200 μmol/L (or 6.4 mg/L). The oxygen consumption rates of TMJ disc explants were measured in a stirred, water-jacketed chamber maintained at 37°C (Instech Laboratories, Plymouth Meeting, PA) [Fig. 2(A)]. After the chamber was sealed, real time dissolved oxygen concentration in the medium was recorded by a fiber optic oxygen sensor (Ocean Optics, Dunedin, FL) until the oxygen concentrations fell to 0.95 μmol/L (0.1% oxygen). At the end of the experiments, the glucose concentration and pH of the culture medium were measured. The decrease in glucose concentration and the change of pH were found to be minimal. In addition, the explant pieces were fully digested and the cell viability was examined via trypan blue exclusion (greater than 90% viability).

A typical plot of dissolved oxygen concentration over time is shown in Fig. 2(B). The rate of oxygen consumption in the TMJ disc cells enclosed in the metabolism chamber can be calculated from the recorded decrease in oxygen concentration versus time. Based on our pilot study, the relationship between the oxygen consumption rate and oxygen concentration can be expressed using the Michaelis-Menten equation:

$$R = \frac{V_{\max} \times C}{K_m + C} \quad (1)$$

where R is oxygen consumption rate (μmol/mL tissue/hr), V_{\max} is the maximum oxygen consumption rate (μmol/mL tissue/hr), K_m is the Michaelis-Menten constant (μmol/L), and C is the oxygen concentration in the chamber (μmol/L). Based on the conservation of mass, the time rate of oxygen concentration change (dC/dt) in the sealed chamber is given by:

$$\frac{dC}{dt} = - \frac{1000V_{\max}C}{K_m + C} \cdot \frac{Vol_{tissue}}{Vol_{chamber}} \quad (2)$$

where Vol_{tissue} is the tissue volume of the explant (mL), $Vol_{chamber}$ is the volume of the metabolism chamber (mL). In this study, the chamber volume is 0.5mL. Integrating Equation 2, we can determine the oxygen concentration in the chamber over the time:

$$t = \frac{K_m}{1000V_{\max} Vol_{tissue} / Vol_{chamber}} \ln \left(\frac{C_0}{C} \right) + \frac{C_0 - C}{1000V_{\max} Vol_{tissue} / Vol_{chamber}} \quad (3)$$

where C_0 is the initial ($t=0$) oxygen concentration in the chamber. Curve-fitting the recorded oxygen concentration data to Equation 3, we determined the kinetic coefficients V_{max} and K_m to establish the functional relationship between the oxygen consumption rate R and the oxygen concentration C . Each measured volume based V_{max} was then normalized by the mean values for cell density in the 5 disc regions obtained from the confocal experiment to calculate the cell based V_{max} .

Statistical analysis

The measurements were presented as mean with 95% confidence interval. The cell density ($n=5$), tissue volume based oxygen consumption rate ($n=4$), and cell based oxygen consumption rate ($n=4$) were examined for significant differences between the five TMJ disc regions using SPSS statistical software. For the volume/cell based oxygen consumption rate, note that the mean value of the left and right TMJ discs was used to represent a single animal, resulting in 4 independent observations. One-way ANOVA and Tukey's post hoc tests were performed to determine if significant differences existed between regions and were reported at p -values < 0.05 .

RESULTS

Distribution of cell density

The surface-regional distribution of the volume based cell density in porcine TMJ discs was determined *in situ* using confocal microscopy techniques. Confocal assessment yielded an overall cell density (mean, 95% CI) of $51.3(21.3-81.3) \times 10^6$ cells/mL in wet tissue. Surface-regional variations in cell density along the superoinferior, anteroposterior, and mediolateral axes are depicted in Table 1. Along the 3 axes, statistically significant differences in total cell numbers were observed only along the anteroposterior and mediolateral axes, with no statistical difference between layers along the superoinferior axis. Although there was no statistically significant difference along the superoinferior axis, the cell density in the middle layer was lower than in the superior and inferior layers. Along the anteroposterior axis, the anterior band had 25.5% higher cell density than the intermediate zone ($p < 0.02$) and 29.1% higher than the posterior band ($p < 0.008$), with no significant difference between the intermediate and posterior band. Along the mediolateral axes, the medial region had 26.2% higher cell density than the intermediate zone ($p < 0.04$) and 25.4% higher than the lateral region ($p < 0.045$), although there was no significant difference between the intermediate zone and lateral region.

Cell density validation using DNA assays

The total DNA content in the TMJ disc was $0.42(0.32-0.518)$ mg/mL in wet tissue. Correspondingly, the cell density across the disc was calculated as $54.6(42.4-66.7) \times 10^6$ cells/mL wet tissue. The comparison of cell density between the confocal microscopy technique and DNA assay is shown in Fig. 3. The cell densities measured by the DNA assay was comparable to the measurements of the confocal technique. There were no significant differences between the two methods for cell density measurements in any of the five regions.

Oxygen consumption rate

A typical curve-fit of the recorded oxygen concentration data with Equation 3 is shown in Fig. 2(B). Good agreement was found between the experimental data and theoretical curve-fitting with $R^2 = 0.989 \pm 0.007$ ($n=40$), indicating that the relationship between the oxygen consumption rate and oxygen concentration can be well expressed using the Michaelis-Menten equation with the two parameters V_{max} and K_m . The V_{max} is the maximum oxygen

consumption rate at high oxygen tension, and the K_m is the oxygen tension at which the oxygen consumption rate decreases to 50% of the V_{max} [Fig. 2(C)]. The overall tissue volume based V_{max} was 1.44(0.44–2.44) $\mu\text{mol}/\text{mL}$ wet tissue/hr. One-way ANOVA showed that the volume based V_{max} was significantly region-dependent ($p < 0.02$). The medial region had the highest, while the anterior had the lowest regional consumption rate (Table 2). There was no significant difference between the medial, intermediate, and lateral regions, as well as between the anterior and posterior bands. However, the averaged volume based V_{max} of central regions [1.69(0.55–2.83) $\mu\text{mol}/\text{mL}$ wet tissue/hr], including intermediate, lateral, and medial, was 76% higher than the averaged value of the anterior and posterior bands [0.96(0.39–1.53) $\mu\text{mol}/\text{mL}$ wet tissue/hr]. The overall K_m was 19.1(13.6–24.6) $\mu\text{mol}/\text{L}$ with no significant regional differences found.

The cell based V_{max} was calculated by normalizing each volume based V_{max} with the corresponding regional mean value for cell density obtained from confocal microscopy. The overall cell based V_{max} was 28.7(12.2–45.2) $\text{nmol}/10^6$ cells/hr. Compared to the volume based V_{max} , region-dependency was further enhanced in the cell based V_{max} ($p < 0.005$) with similar trends of regional distribution (Table 2). The average cell based V_{max} of central regions [34.4(13.6–55.2) $\text{nmol}/10^6$ cells/hr], including intermediate, lateral, and medial, was 72% higher than the averaged value of anterior and posterior bands [20.0(7.8–32.2) $\text{nmol}/10^6$ cells/hr].

The relationships between the oxygen consumption rate and oxygen concentration in the five disc regions are plotted in Fig. 4(A) using the Michaelis-Menten equation with averaged V_{max} and K_m . The oxygen consumption rate was relatively constant and fairly independent of oxygen tension until the oxygen tension fell below 5%. Below 5% oxygen, the rate fell in a highly concentration-dependent manner. Based on the Michaelis-Menten equation, the sensitivity of the oxygen consumption rate to the oxygen tension is solely controlled by the parameter K_m . Using the averaged K_m (19.1 $\mu\text{mol}/\text{L}$) of this study, the oxygen consumption rate relative to that at 21% oxygen tension (1% oxygen = 9.5 $\mu\text{mol}/\text{L}$) was shown in Fig. 4(B). The relative oxygen consumption rate was 0.91 at 10% oxygen, 0.78 at 5% oxygen, 0.55 at 2% oxygen, and 0.36 at 1% oxygen.

DISCUSSION

Since the normal adult human TMJ disc is avascular^{5–7}, the consumption rate of the embedded cell population will be a key determinant of nutrient concentrations within the tissue. The objective of this paper was to determine the basal oxygen consumption rate in porcine TMJ discs using tissue explants and further examine the effects of disc region and oxygen tension on those rates. Recent studies have shown that the oxygen consumption of isolated articular chondrocytes increases with *in vitro* culture duration³⁹. Oxygen consumption increased exponentially in that previous study within the first week and had doubled within the first 24 hours. The increase in oxygen consumption capacity could not be negated by culturing the cells under reduced oxygen atmospheres (2% and 5% O_2), thought to fall within the physiological range of oxygen tensions⁴⁰. Therefore, in this study, fresh TMJ disc explants were used to determine baseline oxygen consumption rates at the physiological glucose concentration of 5mM.

In using tissue explants, it became necessary to measure the distribution of volume based cell density to determine the oxygen consumption rate on a per-cell basis. Conventional histology slices can only provide cell numbers per unit area³⁶. Although enzymatic cell isolation can determine cell numbers per tissue volume, the sequential enzymatic digestion may lose a significant amount of cells⁴¹. Therefore in this study, a confocal microscopy based technique was developed to determine the *in situ* surface-regional cell distribution of

the TMJ disc. The confocal measurements were performed in three layers (i.e., superior, middle, and inferior) for each disc region. Multiple cell layers were found in each 3D confocal imaging data set. Therefore, the confocal measurement did provide real volume based cell number for each disc region. The confocal assessment yielded an overall cell density of $51.3(21.3-81.3) \times 10^6$ cells/mL wet tissue in porcine TMJ disc. Our validation assessment using DNA content yielded the overall cell density of $54.6(42.4-66.7) \times 10^6$ cells/mL. Those values are comparable to the cell density of 50×10^6 cells/mL for porcine TMJ discs using a DNA assay in the literature³⁸. However, complete enzymatic digestion of the bovine TMJ disc yielded a cell density of 20×10^6 cells/mL wet tissue (assuming wet tissue density = 1.08 g/mL)³³. While there is no layer dependency, our results showed that porcine TMJ disc has higher cell density in the anterior and medial regions. This is consistent with the DNA distribution of the porcine TMJ disc in the literature³⁸. Previous qualitative studies have also demonstrated that cells were more numerous in the anterior band compared with the intermediate zone in rabbit and primate TMJ discs⁴²⁻⁴³. One possible explanation is that the peripheral regions have higher cellularity due to a better nutrient supply from surrounding tissues. It is also likely due to an inhomogeneous mechanical strain distribution within the TMJ disc during jaw function. In contrast, a recent study quantitatively indicated that the anterior band has fewer cells than the intermediate zone and posterior band³⁶. Note that the cell density in that study was measured by counting cells on histological slides which cannot be translated for 3D tissue volume based cell density.

The tissue thickness and cell density of the TMJ discs from this study were compared to those of knee joint cartilage in Table 3. Stockwell²⁵ showed that, in general, thinner cartilage has higher cell density than thicker cartilage due to the limitation of nutrient diffusion. The TMJ disc has a bi-concave shape and the thickness of the disc in the superior and inferior direction varies across the surface between 2–4mm. Considering the larger thickness of the TMJ disc, the cell density of TMJ discs is apparently higher than in knee cartilage. This implies that the TMJ disc might have greater demand of nutrients.

The oxygen consumption rate of the TMJ disc was measured in a sealed metabolism chamber. This approach has been used to investigate the effect of oxygen tension on the oxygen consumption rate of isolated articular chondrocytes²⁰ and IVD cells³⁰. Those studies have shown that the relationship between the oxygen consumption rate and oxygen tension can be modeled by the Michaelis-Menten equation with the two parameters V_{max} and K_m . Our results revealed that the kinetics of the oxygen consumption rate of TMJ disc explants can also be well expressed by this equation. Due to small K_m , the oxygen consumption rate of the TMJ disc was relatively constant until the oxygen tension fell below 5%. Below 5% oxygen, the rate fell in a concentration-dependent manner. This finding is similar to the association between the oxygen consumption rate and oxygen concentration for articular cartilage^{20, 28} and IVD³⁰.

The oxygen consumption rates of tissue explants are usually determined at 21% O₂. It is apparent that the tissue volume based oxygen consumption rate of the TMJ disc is the highest among the cartilaginous tissues listed in Table 4A. Although the TMJ disc has a high cell density compared to other cartilage, the maximum cell based oxygen consumption rate (V_{max}) of TMJ disc cells is still about 3 times higher than for articular chondrocytes and IVD cells (Table 4B). Both chondrocytes and IVD cells obtain their energy primarily through Embden-Meyerhof-Parnas (EMP) pathway glycolysis, even in the presence of high oxygen tension^{14, 26-27}. Therefore, the oxygen consumption rate of those cells is exceptionally low. It has even been reported that the mitochondria of chondrocytes *in situ* lack certain cytochromes that are required for a fully functional electron transport chain⁴⁴. Cell morphological studies using electron microscopy have shown that the porcine TMJ disc contains an inhomogeneous distribution of a mixed cell population of fibroblast-like cells

and chondrocyte-like cells, which are distinct from hyaline cartilage chondrocytes³⁶. The chondrocyte-like cells in the TMJ disc do not appear to exhibit the distinct pericellular capsule typical of articular chondrocytes³⁴. Moreover, there are significant differences in organelle content between articular chondrocytes and chondrocyte-like cells in TMJ disc, which likely suggest differences in cellular behavior. The chondrocyte-like cells in TMJ discs have a greater number of mitochondria, suggesting a higher metabolic activity than articular chondrocytes³⁶. The overall higher oxygen consumption rate determined in this study might be related to some extent of oxidative phosphorylation in TMJ disc cells. Detamore *et al.* reported that the distributions of cell subpopulations in TMJ disc are significantly region-dependent³⁶. This might lead to the region-dependent oxygen consumption rate determined in this study. For example, the intermediate zone of the TMJ disc had a higher oxygen consumption rate possibly due to the relatively higher number of chondrocyte-like cells in this region.

Due to the difficulty of measuring nutrient concentrations *in vivo*, mathematical models have been used to evaluate them in cartilaginous tissues. The results of these calculations indicate that there is a steep gradient of oxygen in normal cartilage and the concentration can be as low as 1%²⁰. The normal adult human TMJ disc is a large avascular structure⁵⁻⁷, although some research has shown vasculature in young animal³⁶ and human discs⁴⁵, as well as degenerated human discs⁴⁶. Considering the higher cell density and oxygen consumption rate of TMJ disc cells, a steeper oxygen gradient potentially exists in the normal TMJ disc. Such a steep oxygen gradient would make this tissue uniquely vulnerable to any pathological event which impedes nutrient supply, such as sustained joint loading due to jaw clenching⁴⁷. To precisely predict the nutrient environment using a mathematical model, it is crucial to determine quantitative relationships between the nutrient consumption rates and the local nutrient concentrations. In this study, the relationship between the oxygen consumption rate and oxygen tension was established for the TMJ disc. Studies on articular cartilage and IVD have shown that nutrient consumption rates are dependent not only on a single substrate but also on other nutrients. For instance, stimulation of oxygen uptake at low glucose concentrations (the Crabtree effect) was observed in articular cartilage^{26, 48-50}. The present study only determined the oxygen consumption rate of TMJ disc at 5mM glucose. Therefore, it is necessary to investigate the effect of glucose on the oxygen consumption rate in a future study. It will also be valuable to study the coupling of oxygen consumption, glucose consumption, and lactate production to fully understand the energy metabolism in the TMJ disc.

In summary, the distributions of cell density and basal oxygen consumption rate in five TMJ disc regions were determined using porcine tissue explants. The impact of the oxygen tension on the oxygen consumption rate was investigated and a quantitative relationship between them was established. The TMJ disc had a higher cellularity compared to articular cartilage. The cell density of the TMJ disc was region-dependent, and the anterior and medial regions had higher values compared to intermediate, lateral, and posterior regions. Compared to articular cartilage and IVD, the TMJ disc had a higher oxygen consumption rate on a tissue volume basis, as well as on a per-cell basis. The central regions, including intermediate, lateral, and medial, had a higher average oxygen consumption rate than anterior and posterior bands. The oxygen consumption rate was also dependent on the oxygen tension. At high oxygen tension, the oxygen consumption rate remained constant, and only dropped significantly as oxygen tension fell below 5%. This relationship can be well expressed by the Michaelis-Menten equation. Considering the higher cell density and oxygen consumption rate of TMJ disc cells, a steeper oxygen gradient potentially exists in the normal TMJ disc. Such an oxygen gradient will likely be very vulnerable to any pathological event that can impede nutrient supply, and ultimately result in tissue degeneration.

Acknowledgments

This project was supported by NIH grants DE018741, RR017696, and AR055775, a NSF RII grant fellowship (EPS-00903795) to CS, and a NIH F31 training grant DE020230 to JK.

References

1. Nickel JC, McLachlan KR. In vitro measurement of the stress-distribution properties of the pig temporomandibular joint disc. *Arch Oral Biol.* 1994; 39:439–48. [PubMed: 8060268]
2. Nickel JC, McLachlan KR. In vitro measurement of the frictional properties of the temporomandibular joint disc. *Arch Oral Biol.* 1994; 39:323–31. [PubMed: 8024497]
3. Stegenga B. Osteoarthritis of the temporomandibular joint organ and its relationship to disc displacement. *J Orofac Pain.* 2001; 15:193–205. [PubMed: 11575190]
4. Stegenga B, de Bont LG, Boering G. Osteoarthrosis as the cause of craniomandibular pain and dysfunction: a unifying concept. *J Oral Maxillofac Surg.* 1989; 47:249–56. [PubMed: 2646405]
5. Rees LA. The structure and function of the mandibular joint. *Br Dent J.* 1954; 96:125–33.
6. Leonardi R, Lo ML, Bernasconi G, Caltabiano C, Piacentini C, Caltabiano M. Expression of vascular endothelial growth factor in human dysfunctional temporomandibular joint discs. *Arch Oral Biol.* 2003; 48:185–92. [PubMed: 12648555]
7. Detamore MS, Athanasiou KA. Motivation, characterization, and strategy for tissue engineering the temporomandibular joint disc. *Tissue Eng.* 2003; 9:1065–87. [PubMed: 14670096]
8. Detamore MS, Athanasiou KA. Structure and function of the temporomandibular joint disc: implications for tissue engineering. *J Oral Maxillofac Surg.* 2003; 61:494–506. [PubMed: 12684970]
9. Cernanec J, Guilak F, Weinberg JB, Pisetsky DS, Fermor B. Influence of hypoxia and reoxygenation on cytokine-induced production of proinflammatory mediators in articular cartilage. *Arthritis Rheum.* 2002; 46:968–75. [PubMed: 11953974]
10. Gray ML, Pizzanelli AM, Grodzinsky AJ, Lee RC. Mechanical and physiochemical determinants of the chondrocyte biosynthetic response. *J Orthop Res.* 1988; 6:777–92. [PubMed: 3171760]
11. Grimshaw MJ, Mason RM. Bovine articular chondrocyte function in vitro depends upon oxygen tension. *Osteoarthritis Cartilage.* 2000; 8:386–92. [PubMed: 10966846]
12. Grimshaw MJ, Mason RM. Modulation of bovine articular chondrocyte gene expression in vitro by oxygen tension. *Osteoarthritis Cartilage.* 2001; 9:357–64. [PubMed: 11399100]
13. Henrotin Y, Kurz B, Aigner T. Oxygen and reactive oxygen species in cartilage degradation: friends or foes? *Osteoarthritis. Cartilage.* 2005; 13:643–54.
14. Lee RB, Urban JP. Evidence for a negative Pasteur effect in articular cartilage. *Biochem J.* 1997; 321 (Pt 1):95–102. [PubMed: 9003406]
15. Martin G, Andriamanalijaona R, Grassel S, Dreier R, Mathy-Hartert M, Bogdanowicz P, et al. Effect of hypoxia and reoxygenation on gene expression and response to interleukin-1 in cultured articular chondrocytes. *Arthritis Rheum.* 2004; 50:3549–60. [PubMed: 15529381]
16. Ysart GE, Mason RM. Responses of articular cartilage explant cultures to different oxygen tensions. *Biochim Biophys Acta.* 1994; 1221:15–20. [PubMed: 8130272]
17. Tojyo I, Yamaguchi A, Nitta T, Yoshida H, Fujita S, Yoshida T. Effect of hypoxia and interleukin-1beta on expression of tenascin-C in temporomandibular joint. *Oral Dis.* 2008; 14:45–50. [PubMed: 18173448]
18. Yamaguchi A, Tojyo I, Yoshida H, Fujita S. Role of hypoxia and interleukin-1beta in gene expressions of matrix metalloproteinases in temporomandibular joint disc cells. *Arch Oral Biol.* 2005; 50:81–87. [PubMed: 15598420]
19. Haselgrove JC, Shapiro IM, Silverton SF. Computer modeling of the oxygen supply and demand of cells of the avian growth cartilage. *Am J Physiol.* 1993; 265:C497–C506. [PubMed: 8368277]
20. Zhou S, Cui Z, Urban JP. Factors influencing the oxygen concentration gradient from the synovial surface of articular cartilage to the cartilage-bone interface: a modeling study. *Arthritis Rheum.* 2004; 50:3915–24. [PubMed: 15593204]

21. Zhou S, Cui Z, Urban JP. Nutrient gradients in engineered cartilage: metabolic kinetics measurement and mass transfer modeling. *Biotechnol Bioeng.* 2008; 101:408–21. [PubMed: 18727036]
22. Malda J, Rouwkema J, Martens DE, Le Comte EP, Kooy FK, Tramper J, et al. Oxygen gradients in tissue-engineered PEGT/PBT cartilaginous constructs: measurement and modeling. *Biotechnol Bioeng.* 2004; 86:9–18. [PubMed: 15007836]
23. Stairmand JW, Holm S, Urban JP. Factors influencing oxygen concentration gradients in the intervertebral disc. A theoretical analysis. *Spine.* 1991; 16:444–49. [PubMed: 2047917]
24. Huang CY, Gu WY. Effects of mechanical compression on metabolism and distribution of oxygen and lactate in intervertebral disc. *J Biomech.* 2008; 41:1184–96. [PubMed: 18374341]
25. Stockwell, RA. *Biology of Cartilage Cells.* Cambridge, UK: Cambridge University Press; 1979.
26. Otte P. Basic cell metabolism of articular cartilage. Manometric studies. *Z Rheumatol.* 1991; 50:304–12. [PubMed: 1776367]
27. Holm S, Maroudas A, Urban JP, Selstam G, Nachemson A. Nutrition of the intervertebral disc: solute transport and metabolism. *Connect Tissue Res.* 1981; 8:101–19. [PubMed: 6453689]
28. Heywood HK, Knight MM, Lee DA. Both superficial and deep zone articular chondrocyte subpopulations exhibit the Crabtree effect but have different basal oxygen consumption rates. *J Cell Physiol.* 2010; 223:630–39. [PubMed: 20143333]
29. Bibby SR, Jones DA, Ripley RM, Urban JP. Metabolism of the intervertebral disc: effects of low levels of oxygen, glucose, and pH on rates of energy metabolism of bovine nucleus pulposus cells. *Spine (Phila Pa 1976).* 2005; 30:487–96. [PubMed: 15738779]
30. Huang CY, Yuan TY, Jackson AR, Hazbun L, Fraker C, Gu WY. Effects of low glucose concentrations on oxygen consumption rates of intervertebral disc cells. *Spine (Phila Pa 1976).* 2007; 32:2063–69. [PubMed: 17762806]
31. Guehring T, Wilde G, Sumner M, Grunhagen T, Karney GB, Tirlapur UK, et al. Notochordal intervertebral disc cells: sensitivity to nutrient deprivation. *Arthritis Rheum.* 2009; 60:1026–34. [PubMed: 19333932]
32. Ishihara H, Urban JP. Effects of low oxygen concentrations and metabolic inhibitors on proteoglycan and protein synthesis rates in the intervertebral disc. *J Orthop Res.* 1999; 17:829–35. [PubMed: 10632449]
33. Landesberg R, Takeuchi E, Puzas JE. Cellular, biochemical and molecular characterization of the bovine temporomandibular joint disc. *Arch Oral Biol.* 1996; 41:761–67. [PubMed: 9022913]
34. Berkovitz BK, Pacy J. Ultrastructure of the human intra-articular disc of the temporomandibular joint. *Eur J Orthod.* 2002; 24:151–58. [PubMed: 12001551]
35. Detamore MS, Orfanos JG, Almarza AJ, French MM, Wong ME, Athanasiou KA. Quantitative analysis and comparative regional investigation of the extracellular matrix of the porcine temporomandibular joint disc. *Matrix Biol.* 2005; 24:45–57. [PubMed: 15749001]
36. Detamore MS, Hegde JN, Wagle RR, Almarza AJ, Montufar-Solis D, Duke PJ, et al. Cell type and distribution in the porcine temporomandibular joint disc. *J Oral Maxillofac Surg.* 2006; 64:243–48. [PubMed: 16413896]
37. Yao H, Justiz MA, Flagler D, Gu WY. Effects of Swelling Pressure and Hydraulic Permeability on Dynamic Compressive Behavior of Lumbar Annulus Fibrosus. *Annals of Biomed Engng.* 2002; 30:1234–41.
38. Almarza AJ, Bean AC, Baggett LS, Athanasiou KA. Biochemical analysis of the porcine temporomandibular joint disc. *Br J Oral Maxillofac Surg.* 2006; 44:124–28. [PubMed: 16011866]
39. Heywood HK, Lee DA. Monolayer expansion induces an oxidative metabolism and ROS in chondrocytes. *Biochem Biophys Res Commun.* 2008; 373:224–29. [PubMed: 18555010]
40. Heywood HK, Lee DA. Low oxygen reduces the modulation to an oxidative phenotype in monolayer-expanded chondrocytes. *J Cell Physiol.* 2010; 222:248–53. [PubMed: 19795395]
41. Berkovitz BK, Pacy J. The ultrastructure of the intra-articular disc of the temporomandibular joint, with special reference to fibrocartilage. *Bull Group Int Rech Sci Stomatol Odontol.* 1999; 41:2–13. [PubMed: 11799762]

42. Mills DK, Fiandaca DJ, Scapino RP. Morphologic, microscopic, and immunohistochemical investigations into the function of the primate TMJ disc. *J Orofac Pain.* 1994; 8:136–54. [PubMed: 7920350]
43. Scapino RP, Canham PB, Finlay HM, Mills DK. The behaviour of collagen fibres in stress relaxation and stress distribution in the jaw-joint disc of rabbits. *Arch Oral Biol.* 1996; 41:1039–52. [PubMed: 9068868]
44. Mignotte F, Champagne AM, Froger-Gaillard B, Benel L, Gueride M, Adolphe M, et al. Mitochondrial biogenesis in rabbit articular chondrocytes transferred to culture. *Biol Cell.* 1991; 71:67–72. [PubMed: 1912949]
45. Mah J. Histochemistry of the foetal human temporomandibular joint articular disc. *Eur J Orthod.* 2004; 26:359–65. [PubMed: 15366379]
46. Yoshida H, Fujita S, Nishida M, Iizuka T. Localization of lymph capillaries and blood capillaries in human temporomandibular joint discs. *J Oral Rehabil.* 1999; 26:600–7. [PubMed: 10445480]
47. Milam SB. Pathogenesis of degenerative temporomandibular joint arthritides. *Odontology.* 2005; 93:7–15. [PubMed: 16170470]
48. Bywaters EGL. The metabolism of joint tissues. *J Pathol Bacteriol.* 1937; 44:247–68.
49. Rosenthal O, Bowei MA, Wagoner G. Studies in the metabolism of articular cartilage I. Respiration and glycolysis of cartilage in relation to its age. *J Cell Physiol.* 1941; 17:221–33.
50. Heywood HK, Bader DL, Lee DA. Rate of oxygen consumption by isolated articular chondrocytes is sensitive to medium glucose concentration. *J Cell Physiol.* 2006; 206:402–10. [PubMed: 16155906]

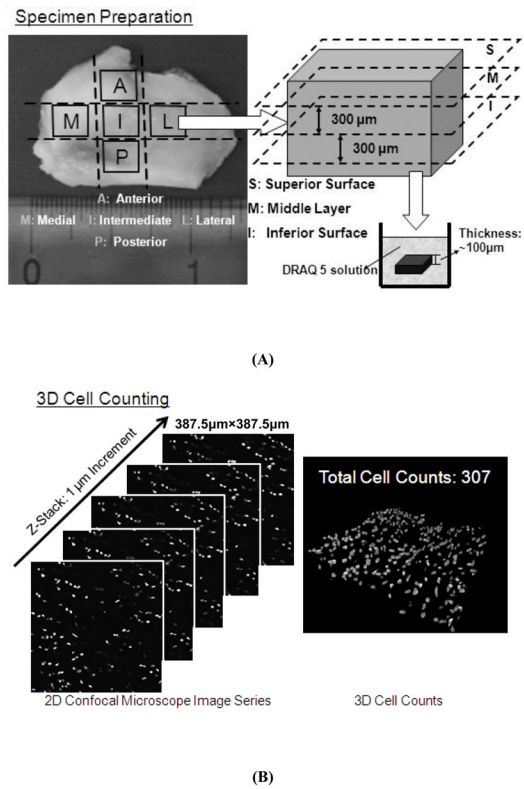
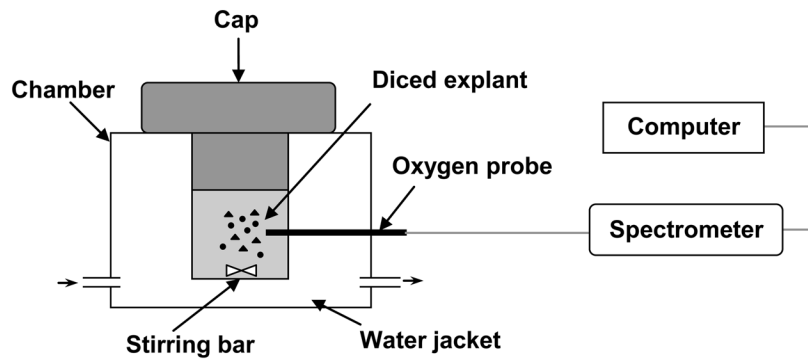
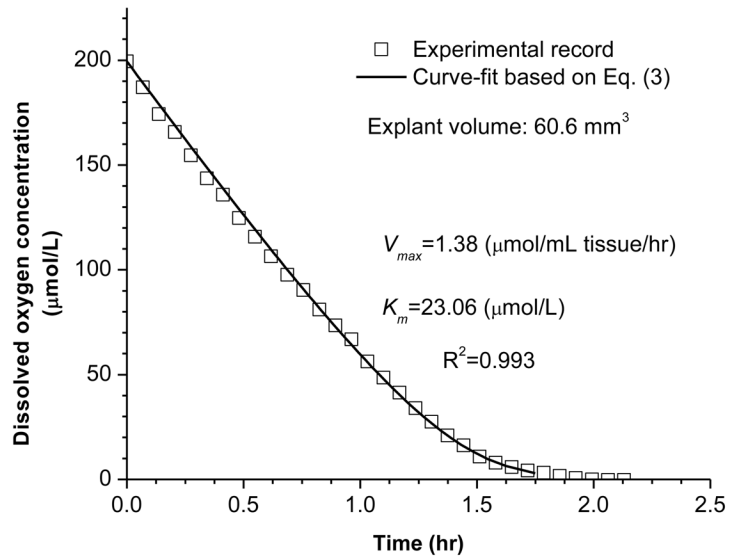


Figure 1.

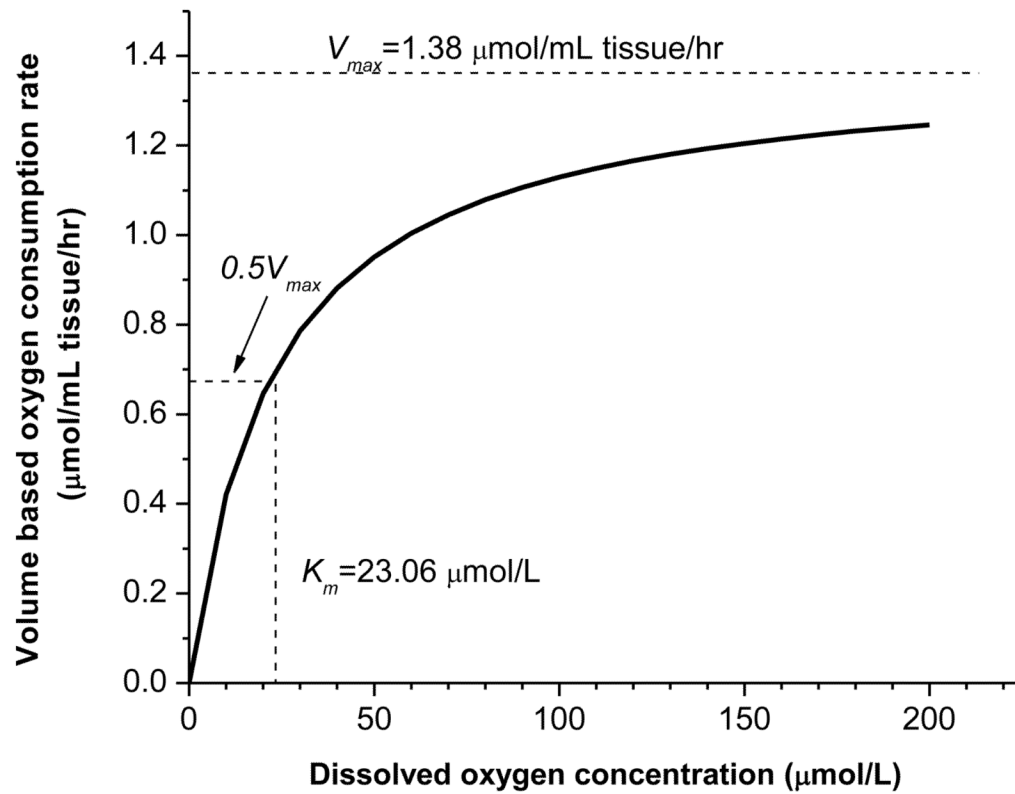
(A) Representation of the regions investigated for determining cell density and oxygen consumption rate. The TMJ disc was divided into five regions: anterior, intermediate, posterior, lateral and medial. From each region, sections (100 μ m) were further taken from 3 layers for cell density measurement. (B) Schematic of 3D cell counting using a confocal microscopy technique.



(A)



(B)



(C)

Figure 2.

(A) Schematic of the experimental setup for oxygen consumption rate measurements. TMJ disc explants were cultured in a sealed water-jacketed metabolism chamber. (B) Typical record of dissolved oxygen concentration in the chamber over time. The experimental data were curve fit to Equation (3). (C) The oxygen consumption rate was plotted based on the Michaelis-Menten equation with determined parameters V_{max} and K_m .

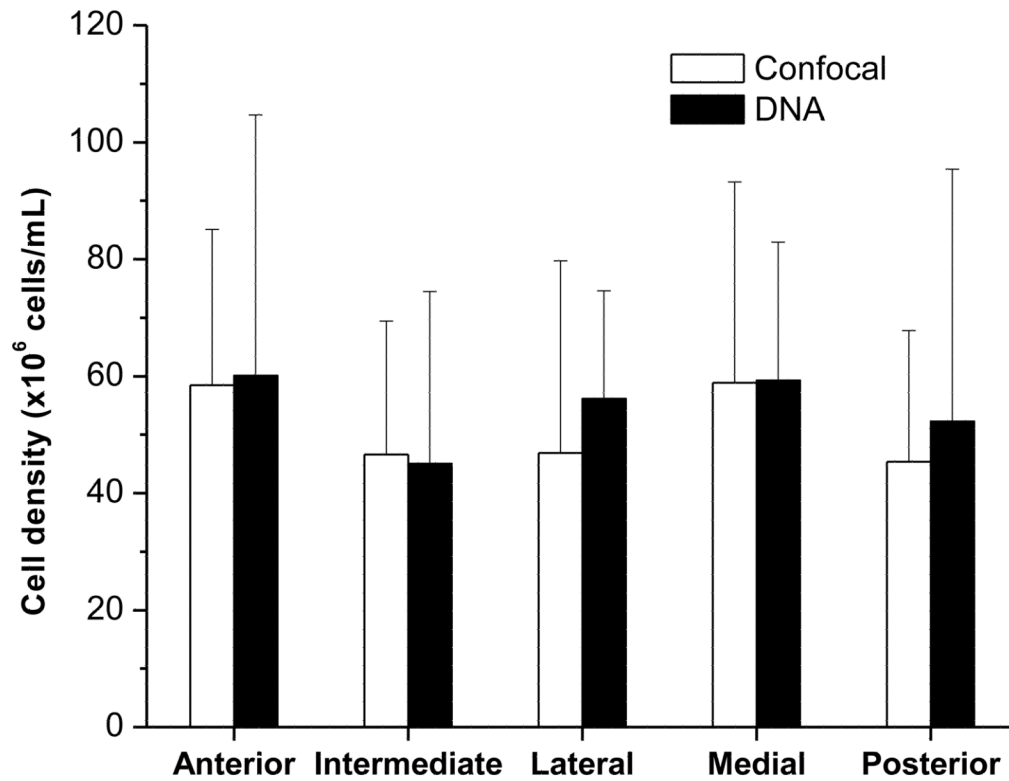
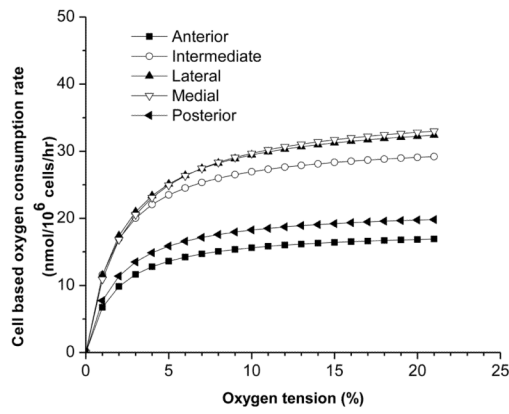
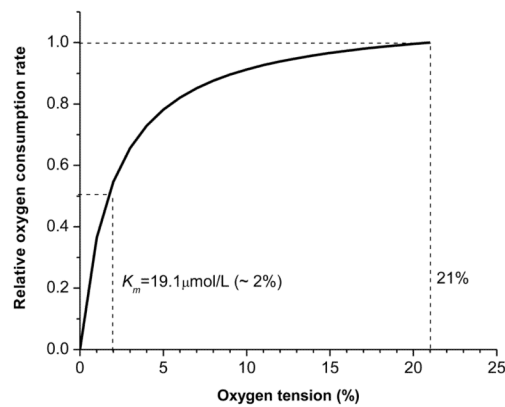


Figure 3. Comparison of cell density between the confocal microscopy technique (n=5) and DNA assay (n=5). The error bar is a 95% confidence interval. No significant differences were detected in each disc region.



(A)



(B)

Figure 4. (A) Relationship between the oxygen consumption rate and the oxygen tension based on the Michaelis-Menten equation with averaged cell based V_{max} and K_m in five disc regions. (B) Predicted relationship between the relative oxygen consumption rate and the oxygen tension. The averaged K_m across the TMJ disc was $19.1 \mu\text{mol/L}$. The oxygen consumption rate was normalized by the rate at 21% oxygen.

Table 1

Surface-regional distribution of cell density (mean, 95% CI): superoinferior direction (n=5, $p=0.415$), anteroposterior direction (n=5, $p<0.01$), and mediolateral direction (n=5, $p<0.04$).

	Surface/Region	Cell density ($\times 10^6$ cells/mL)
Superoinferior	Superior	53.6(20.1–87.1)
	Middle	48.1(22.8–73.4)
	Inferior	52.6(21.6–83.6)
Anteroposterior	Anterior	58.5(31.8–85.2)*
	Intermediate	46.6(23.9–69.3)
	Posterior	45.3(22.8–67.8)
Mediolateral	Medial	58.8(24.5–93.1)*
	Intermediate	46.6(23.9–69.3)
	Lateral	46.9(14.2–79.6)

The symbol (*) indicates significance for the post hoc test ($p<0.05$) in each direction.

Table 2

Regional distribution of oxygen consumption rate (n=4): volume based V_{max} (significantly region-dependent, $p<0.02$), cell based V_{max} (significantly region-dependent, $p<0.005$), and kinetic constant K_m (not significantly region-dependent, $p=0.965$).

	Volume based V_{max} ($\mu\text{mol/mL tissue/hr}$)	Cell based V_{max} ($\text{nmol}/10^6 \text{ cells/hr}$)	K_m ($\mu\text{mol/L}$)
Anterior	0.95(0.28–1.62)	18.3(5.4–31.2)	17.2(5.6–28.8)
Intermediate	1.47(0.19–2.75)	31.6(0.6–62.6)	17.3(4.6–30.0)
Lateral	1.67(0.42–2.92)	35.6(8.4–62.8)*	20.9(4.4–37.4)
Medial	2.16(0.38–3.94)*	36.7(6.5–66.9)*	23.6(13.2–34.0)
Posterior	0.98(0.45–1.51)	21.5(9.9–33.1)	17.8(10.4–25.2)

The symbol (*) indicates significance compared to anterior/posterior bands for the post hoc test ($p<0.05$).

Table 3

Comparison of tissue thickness and cell density between knee articular cartilage and the TMJ disc.

Type of joint and species	Tissue thickness (mm)	Cell density ($\times 10^6$ cells/mL)	Reference
Rabbit knee	0.21	188	[22]
Dog knee	0.67	44.4	[22]
Bovine knee	1.7	19.8	[22]
Human knee	2.3	14.1	[22]
Porcine TMJ disc	2 – 4	51.3	Present study

Table 4A

Comparison of tissue volume based oxygen consumption rate in the TMJ disc and other cartilaginous tissues.

Type of joint and species	Medium glucose (mM)	Volume based oxygen consumption rate ($\mu\text{mol}/\text{mL tissue/hr}$)	Reference
Bovine Knee cartilage	0	0.11	[46]
	10	0.21	[46]
Porcine knee cartilage	0	0.94	[23]
	5	0.45	[23]
	10	0.4	[23]
Bovine AF	n/a	0.68	[29]
Bovine NP	n/a	0.75	[29]
Porcine TMJ disc	5	1.44	Present study

Table 4B

Comparison of cell based oxygen consumption rate between the TMJ disc and other cartilaginous tissues.

Type of joint and species	Subpopulation	Cell based V_{max} consumption rate (nmol/10 ⁶ cells/hr)	K_m (μmol/L)	Reference
Bovine articular chondrocytes	Superficial	3.2	68	[25]
	Deep	6.6	63	[25]
Porcine IVD	AF	6.0	35.7	[27]
	NP	11.5	6.8	[27]
Porcine TMJ disc	Anterior	18.3	17.2	Present study
	Central	34.4	20.6	Present study
	Posterior	21.5	17.8	Present study